J Physiol 587.24 (2009) pp 5925–5938

The Journal of Physiology

Fluctuations in isometric muscle force can be described by one linear projection of low-frequency components of motor unit discharge rates

Francesco Negro[1], Aleš Holobar[2,3] and Dario Farina[1]

[1] *Center for Sensory-Motor Interaction (SMI), Department of Health Science and Technology, Aalborg University, Aalborg, Denmark*
[2] *Laboratorio di Ingegneria del Sistema Neuromuscolare, Politecnico di Torino, Torino, Italy*
[3] *Faculty of Electrical Engineering and Computer Science, University of Maribor, Maribor, Slovenia*

The aim of the study was to investigate the relation between linear transformations of motor unit discharge rates and muscle force. Intramuscular (wire electrodes) and high-density surface EMG (13 × 5 electrode grid) were recorded from the abductor digiti minimi muscle of eight healthy men during 60 s contractions at 5%, 7.5% and 10% of the maximal force. Spike trains of a total of 222 motor units were identified from the EMG recordings with decomposition algorithms. Principal component analysis of the smoothed motor unit discharge rates indicated that one component (first common component, FCC) described 44.2 ± 7.5% of the total variability of the smoothed discharge rates when computed over the entire contraction interval and 64.3 ± 10.2% of the variability when computed over 5 s intervals. When the FCC was computed from four or more motor units per contraction, it correlated with the force produced by the muscle (62.7 ± 10.1%) by a greater degree ($P < 0.001$) than the smoothed discharge rates of individual motor units (41.4 ± 7.8%). The correlation between FCC and the force signal increased up to 71.8 ± 13.1% when the duration and the shape of the smoothing window for discharge rates were similar to the average motor unit twitch force. Moreover, the coefficients of variation (CoV) for the force and for the FCC signal were correlated in all subjects (R^2 range = 0.14–0.56; $P < 0.05$) whereas the CoV for force was correlated to the interspike interval variability in only one subject ($R^2 = 0.12$; $P < 0.05$). Similar results were further obtained from measures on the tibialis anterior muscle of an additional eight subjects during contractions at forces up to 20% of the maximal force (e.g. FCC explained 59.8 ± 11.0% of variability of the smoothed discharge rates). In conclusion, one signal captures most of the underlying variability of the low-frequency components of motor unit discharge rates and explains large part of the fluctuations in the motor output during isometric contractions.

(Received 15 July 2009; accepted after revision 16 October 2009; first published online 19 October 2009)
Corresponding author D. Farina: Center for Sensory-Motor Interaction (SMI), Department of Health Science and Technology, Aalborg University, Fredrik Bajers Vej 7 D-3, DK-9220 Aalborg, Denmark. Email: df@hst.aau.dk

Abbreviations CIS, common input strength; CoV, coefficients of variation; FCC, first common component; MVC, maximal voluntary contraction; PCA, principal component analysis.

Introduction

The central nervous system controls the force generated by a muscle through a size-governed recruitment (Henneman *et al.* 1965) and modulation of the discharge rate of the motor neuron pool (Person & Kudina 1972; Milner-Brown *et al.* 1973). The motor neuron is the controller of a transducer (the motor unit) that converts synaptic input into contraction force (Heckman & Enoka, 2004). Only the low-frequency components of the neural drive are reflected in the motor output of this transducer (Mannard & Stein, 1973). Thus, the low-frequency component of the neural drive to the muscle constitutes the effective control signal.

Descending and sensory inputs have several divergent projections to α-motor neurons (Ishizuka *et al.* 1979; Lawrence *et al.* 1985). These common inputs induce a correlation between the low-frequency oscillations in discharge rates of motor neurons, which has been termed *common drive* (De Luca *et al.* 1982). The presence of

DOI: 10.1113/jphysiol.2009.178509

common low-frequency components in the discharge rates of motor units has been observed in sustained contractions of muscles of the lower and upper limbs (De Luca & Erim, 2002; De Luca *et al.* 2009).

The common modulation of motor unit discharge rates can be quantified by the peak value of the cross-correlation function between the smoothed discharge rates of pairs of motor units (De Luca *et al.* 1982). This analysis does not assess the overall level of common low-frequency activity of the motor neuron pool, but it is limited to pairs of motor units serially analysed. The approach is justified by the relatively small number of motor units that can be usually detected *in vivo* during voluntary contractions. Since only low-frequency components of the neural drive to the muscle are reflected in the motor output and the modulation of discharge rate of the motor neuron pool is mainly controlled by a largely spread synaptic input (Ralston *et al.* 1984, Lemon & Mantel, 1989), in this study, it is hypothesized that the effective drive to the muscle can be described by a low-dimensional signal, extracted from the correlated activity of the population of active motor units. This signal should be sufficient to explain the majority of the variability in the generated force.

In this study we investigated *in vivo* the discharge rates of human motor units by principal component analysis (PCA) (Joliffe & Morgan, 1992). The principal components of a set of signals are uncorrelated with respect to each other, and their power expresses the percentage of variance that each component contributes to that set of signals. Thus, when applied to smoothed motor unit discharge rates, this analysis allows the investigation of the dimensionality of the control for a population of motor units. Moreover, since the principal components of a multivariate measure reflect common variability of the given set of signals, it is expected that they are optimally representative of the motor output that is likely to be mostly affected by the common components.

Therefore, the aim of the study was to identify a common signal component by linear transformation of the low-frequency oscillations of motor unit discharge rates and to investigate its relation with the force fluctuations expressed by the muscle. The analyses were performed on a small hand muscle, the abductor digiti minimi, and on a larger muscle of the leg, the tibialis anterior muscle. The results are reported in detail for the abductor digiti minimi muscle, whereas only the main findings are reported for the tibialis anterior muscle. Preliminary results have been presented in abstract form (Negro & Farina, 2008; Holobar *et al.* 2009*b*).

Methods

The experiments were performed on two groups of eight healthy men on the abductor digiti minimi (mean ± S.D., age: 27.0 ± 3.5 years; range, 22–32 years) and the tibialis anterior muscle (mean ± S.D., age: 25.3 ± 1.8 years; range, 23–28 years). The experiments were conducted in accordance with the *Declaration of Helsinki* and approved by the ethics committee of Region Nordjylland, Denmark (approval number N-20090019). All participants signed a written informed consent form before inclusion. The experimental procedures were the same for the two muscles, unless otherwise indicated.

EMG recordings

Single motor unit action potentials were recorded with intramuscular and surface EMG (Fig. 1*B* and *C*). Intramuscular EMG was measured using Teflon-coated stainless steel wires (diameter 0.1 mm; A-M Systems, Carlsborg, WA, USA) inserted with 25-gauge hypodermic needles. To identify a relatively large number of motor units per contraction, two pairs of wires were placed approximately 1 cm apart in the transverse direction in the proximal portion of each of the muscles investigated. The needles were inserted and removed after insertion, leaving the wires inside the muscle. Each wire was cut to expose the cross section of the tip without insulation. The two bipolar intramuscular EMG signals were amplified (Counterpoint EMG, Dantec Medical, Skovlunde, Denmark), band-pass filtered (500 Hz to 5 kHz), and sampled at 10 kHz (Fig. 1*B*). The position of the wires was slightly adjusted before starting the recordings and when the signal quality was poor, which occurred rarely, a new pair of wires was inserted.

Surface EMG signals were recorded with 13 × 5 electrode grids (Aalborg University, Denmark, and Politecnico di Torino, Italy) with 2.5 mm and 5 mm of interelectrode spacing for the abductor digiti minimi and tibialis anterior muscle, respectively. The grids were located over the distal portion of each muscle. Before the placement of the grid, the skin was lightly abraded using abrasive paste (Meditec–Every, Parma, Italy) and cleansed afterward. The surface EMG signals were amplified as bipolar recordings along the direction of the fibres (LISiN-OT Bioelettronica, Torino, Italy), band-pass filtered (3 dB bandwidth, 10–500 Hz), and sampled at 2048 Hz by 12-bit A/D converter.

Procedures

For the measures on the abductor digiti minimi, the subject was seated on an adjustable chair with the right arm extended in a force brace (Aalborg University). The fifth finger was fixed in the isometric device for measurement of finger-abduction forces. The forearm and the four digits were secured with Velcro straps. The force produced by the fifth finger was measured using two force

transducers (Interface Inc., Scottsdale, AZ, USA), one in the transverse plane (abduction force) and the other in the sagittal plane (flexion force) (Fig. 1*A*). For the measures on the tibialis anterior, the subjects were seated on a chair with the foot fixed in an isometric brace for the measure of ankle dorsiflexion torque (Aalborg University). The force signal was sampled at 10 kHz and stored on a computer. Visual feedback on the finger abduction or ankle dorsiflexion force was provided on an oscilloscope.

The subjects performed three maximal voluntary contractions (MVCs) of the target muscle with a rest of 2 min in between. The maximum force achieved during the maximal contractions was considered as the reference MVC. Five minutes after the MVCs, the subject performed three contractions of 60 s duration at 5%, 7.5% and 10% MVC (abductor digiti minimi) or 10%, 15% and 20% MVC (tibialis anterior), in random order. The levels for force were chosen in order to be confident of the accuracy of decomposition, as investigated in preliminary tests. The EMG signal complexity was greater for the abductor digiti minimi than the tibialis anterior for similar force levels, and thus the maximum force level investigated could be slightly higher for the tibialis anterior muscle. However, one of the investigated force levels (10% MVC) was chosen in common for the two muscles for direct comparison of the results. Prior to each sustained contraction, the subject performed two contractions in which the force increased linearly from 0% to the target force of the subsequent sustained contraction in 10 s (ramp contractions). The two ramp contractions were separated by 30 s of rest and the subject further rested for 2 min between the second ramp contraction and the subsequent sustained contraction and for 5 min after each sustained contraction. The subject had feedback on force during all contractions. During each contraction of the abductor digiti mimini, the flexion force was monitored and contractions during which this force was not negligible were repeated.

EMG signal decomposition

The action potentials of individual motor units were identified from the intramuscular EMG signals recorded from the two locations in the muscle by the use of a decomposition algorithm (McGill *et al.* 2005). Each motor unit spike train was manually edited by an experienced operator and any unusually long (>250 ms) or short (<20 ms) inter-spike intervals (ISIs) were manually inspected to check for potential discrimination errors. The surface EMG was decomposed with the convolution kernel compensation (CKC) technique (Holobar & Zazula,

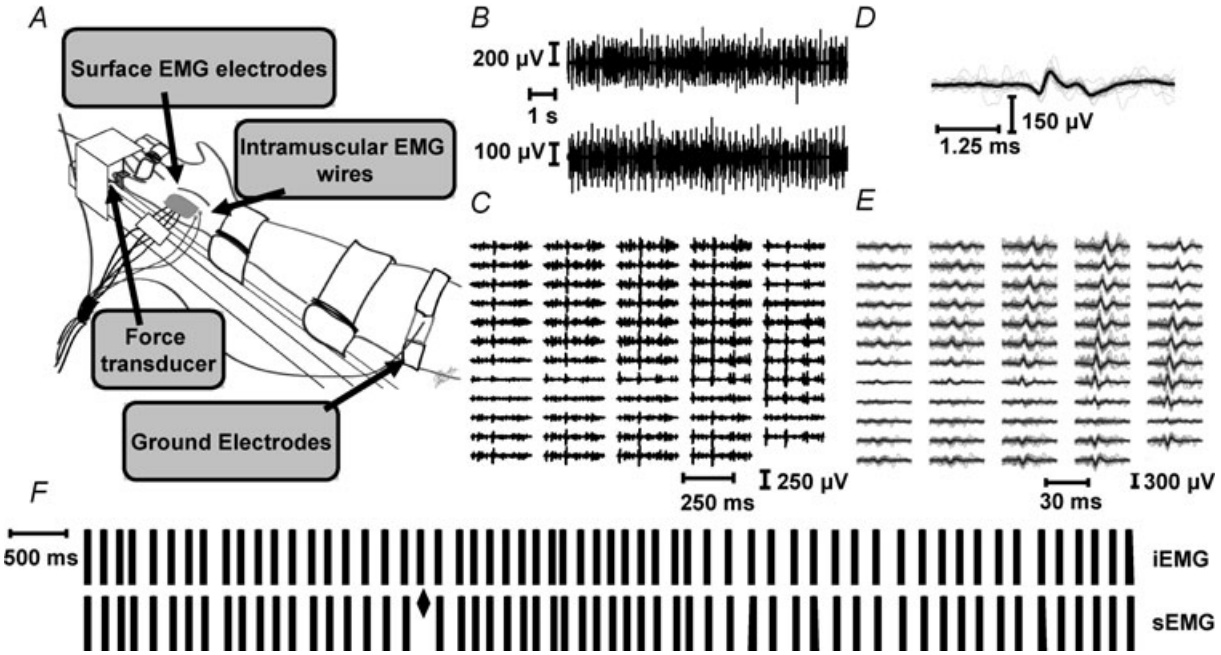

Figure 1. Experimental set-up and representative recordings for the abductor digiti minimi muscle
A, force measurement from the abductor digiti minimi muscle. *B*, intramuscular EMG recorded from two locations in the abductor digiti minimi. *C*, surface EMG recorded with 64 electrodes resulting in 59 bipolar derivations. *D*, intramuscular action potentials of a motor unit identified from one of the intramuscular EMG signals. *E*, surface action potentials of the same motor unit shown in *D*. *F*, comparison between the spike trains identified from intramuscular EMG (iEMG) and surface EMG (sEMG) decomposition for the motor unit shown in *D* and *E* (the diamond indicates the disagreement between the two decomposition techniques). The contraction force was 10% MVC.

2004; Holobar *et al.* 2009*a*) and manually verified by an experienced operator.

Because the analysis of common components in motor unit discharge rates is sensitive to errors in the estimation of the spike trains and requires a relatively large motor unit sample, an analysis of decomposition accuracy was performed for each motor unit which was detected concurrently by at least two recording systems (Fig. 1*D* and *F*). The discharge times detected from two signals were compared using a time tolerance of ±0.5 ms. The number of discharge times identified by two systems within the set tolerance, as a percentage of the total number of discharge times, was considered an indication of the number of correctly detected action potentials (Mambrito & De Luca, 1984). Concurrent erroneous identification of two discharges by two independent recording and decomposition techniques is indeed very unlikely (Mambrito & De Luca, 1984). This provided a lower limit to the accuracy of the decomposition methods in the present experimental conditions.

Signal and data analysis

The envelope of the surface EMG signal was computed from the channel in the central location of the grid by filtering the rectified EMG with a Hann window of duration 400 ms.

The recruitment threshold of the motor units was measured from the ramp contractions that preceded each sustained contraction and corresponded to the force level of the first motor unit discharge, excluding discharges that were separated from the next for <40 ms or >200 ms (Farina *et al.* 2009). The difference ΔFR between the recruitment threshold of a motor unit and the target force in each sustained contraction was computed.

The instantaneous discharge rates of each motor unit were smoothed using a Hann window of duration 400 ms and high-pass filtered with cut-off frequency 0.75 Hz (zero-phase filter, $H(f) = 1 - \frac{\sin(\pi f)}{\pi f}$) to remove offsets and trends, as proposed in previous studies (De Luca *et al.* 1982). The resulting smoothed and detrended discharge rates (later referred to for simplicity only as smoothed discharge rates) were arranged in a matrix (time samples × motor unit) and their principal components were computed using the eigenvalue decomposition of their covariance matrix (Joliffe & Morgan, 1997):

$$\Sigma = \begin{pmatrix} E[X_1X_1] & E[X_1X_2] & \dots & E[X_1X_N] \\ E[X_2X_1] & E[X_2X_2] & \dots & E[X_2X_N] \\ \vdots & \vdots & \ddots & \vdots \\ E[X_NX_1] & E[X_NX_2] & \dots & E[X_NX_N] \end{pmatrix}, \quad (1)$$

where $E[X_iX_i]$ and $E[X_iX_j]$, with $i \neq j$, are the auto- and cross-covariance of the smoothed discharge rates of the i-th and j-th motor units. The term $E[X_iX_j]$ is equivalent to the cross-correlation between pairs of smoothed discharge rates, which is the measure of common drive proposed by De Luca *et al.* (1982). The lower bound for the maximum eigenvalue of the covariance matrix is (Walker & Van Mieghem, 2008):

$$\lambda_{\max} \geq \frac{\sum_{i,j} E\left[X_iX_j\right]}{N} = \frac{\sum_{i} E\left[X_iX_i\right] + \sum_{i \neq j} E\left[X_iX_j\right]}{N} \quad (2)$$

In this study, the maximum eigenvalue of the covariance matrix, which corresponds to the relative power of the first principal component, was used to quantify the strength of the common low-frequency oscillations in the activities of the identified motor units. Moreover, we analysed the characteristics of the first principal component signal. The first principal component is a signal that projects the largest common variations in the smoothed motor unit discharge rates. In the following, we refer to this signal as the 'first common component' (FCC) of the motor unit discharge rates.

For comparison with previous studies, the strength of the association between motor unit discharge rates was also analysed by studying pairs of motor units, as previously proposed (common drive) (De Luca *et al.* 1982). Equation (2) includes a term proportional to the previously proposed common drive index, defined as the average of the peak of the cross-correlation functions between pairs of motor unit discharge rates (De Luca *et al.* 1982):

$$CDI = \frac{\sum_{i \neq j} E\left[X_iX_j\right]}{N(N-1)} \quad (3)$$

The strength of the common drive was computed over intervals of 5 s duration using eqn (3) and averaged over the contraction duration, with the same pre-processing on discharge rates as described above for computing the principal components. Only peak values of the cross-correlation function corresponding to time delays in the interval ± 100 ms were considered for this analysis, as previously suggested (De Luca & Erim, 2002).

The degree of motor unit short term synchronization was calculated using the cross-correlation histograms (bin width: 1 ms) between −100 ms prior to and 100 ms after the discharge of the reference unit (Nordstrom *et al.* 1992). The cumulative sum (CUSUM) technique was used to assess the location of the peak of the histograms, as described previously (Ellaway, 1978; Davey *et al.* 1986; Semmler *et al.* 1997). The strength of short-term synchronization was measured as the common input strength (CIS) index, defined by Nordstrom *et al.* (1992).

CIS values reported in the results are the average over all pairs of motor units identified for each contraction (Semmler & Nordstrom, 1999).

The coefficients of variation (CoV) for the ISI, for the force signal and for the envelope of the surface EMG were computed as the ratio (%) between the S.D. and the mean values, after removal of the linear trends. The CoV for the FCC signal was computed in a similar way, as the ratio between the S.D. of the detrended FCC signal and its mean value. For all the variables, the CoV was computed using intervals of 4 s duration and the values obtained were averaged over the contraction duration.

The associations between force, the FCC signal and the envelope of the surface EMG were analysed with cross-correlation (time-domain) and coherence (frequency-domain) analyses. Coherence spectra were estimated from the magnitude squared of the cross spectrum and normalized by the product of the auto-spectra. The spectra and cross-spectra were computed from intervals of 2 s duration and then averaged over the entire signal duration. The coherence level was considered significant when it was greater than the 95% confidence limit.

Statistical analysis

All variables were analysed with the Kolmogorov–Smirnov test to check the assumption of standard normal distribution. Since this test indicated normal distribution for all the variables, parametric statistical analyses were used.

Student's *t* test for paired data was used to compare the discharge rates at the beginning and the end of each contraction. One-way ANOVA was used to compare the recruitment threshold and ΔFR among contraction levels. One-way ANOVA was also used to analyse the relative power of the FCC signal and the strength of correlation between FCC and force when varying the number of motor units used for the principal component analysis. Pair-wise comparisons were performed by the Student–Newman–Keuls *post hoc* test when ANOVA was significant.

Linear regression analysis was used to assess the relation between the common drive index computed for pairs of motor units as in eqn (3) (De Luca *et al.* 1982) and the relative power of the FCC signal (largest eigenvalue of the covariance matrix in eqn (1)). Regression analyses were also performed to determine the association between the CoV for the FCC and either the CoV for force or for the envelope of the surface EMG. Moreover, linear regression analysis was used to investigate the following associations: CoV for ISI *vs.* ΔFR, mean motor unit discharge rate *vs.* ΔFR, and CoV for ISI *vs.* CoV for force.

Data are reported as means and S.D. Significance was accepted for *P*-values less than 0.05.

Results

Detailed results are reported for the abductor digiti minimi muscle, whereas, in a summary table, only the most relevant results are reported for the tibialis anterior muscle. The measurements on the tibialis anterior muscle served to prove that the main conclusions can be generalized to muscles larger than the abductor digiti minimi and to greater forces. Unless specified otherwise, the following results refer to the abductor digiti minimi muscle.

During the 60 s contractions, a range of 0–3 motor units not active at the beginning of the contractions were recruited during the contractions. Recruitment occurred after (range) 22–57 s from the beginning of the contraction. The following results are reported only for those units of the abductor digiti minimi that were active for the entire duration of the contraction.

Figure 2 shows an example of identification of motor unit action potentials from two intramuscular signals and surface EMG. In this example, 14 motor units were identified in total. Three of these motor units were identified concurrently from one of the intramuscular signals and the surface EMG. From the group data, 28 motor units (range 0–5) were identified concurrently by the two intramuscular detection systems and for these units the level of agreement in decomposition was (average over all contraction forces) $97.9 \pm 1.3\%$ (Table 1). Moreover, 29 motor units (range 0–3) were identified concurrently from at least one intramuscular recording site and the surface EMG, with agreement in decomposition of (average over all contraction forces) $93.7 \pm 5\%$ of discharges (Table 1). Therefore, the decomposition procedures were highly accurate.

After merging the motor units detected by more than one detection system, 222 motor units were identified from the 24 recordings from the abductor digiti minimi muscle (8 subjects $\times$ 3 contraction forces). Thus, on average $\sim$9 motor units per contraction could be investigated with a high level of accuracy (>93%), which was necessary for the population analysis performed in the following.

The average discharge rate of the identified motor units showed a decline over time during the 60 s contractions, although this was not significant (average over all contraction forces, 12.7 ± 2.2 pps and 12.2 ± 2.3 pps for the first and last 10 s of activity, $P > 0.05$; Table 2). The recruitment thresholds of the identified motor units ($3.6 \pm 2.7\%$ MVC) differed among the contraction levels ($P < 0.05$; Table 2). Accordingly, the values of ΔFR ($4.1 \pm 2.5\%$ MVC) increased with contraction force and were different among force levels ($P < 0.001$; Table 2). ΔFR values and CoV for ISI ($18.8 \pm 4.1\%$; Table 2) were not correlated ($R^2 = 0.0001$, $P = 0.64$; Fig. 3*A*) whereas there was a weak but significant correlation between the average discharge rate and ΔFR ($R^2 = 0.04$, $P < 0.05$; Fig. 3*B*).

Table 1. Accuracy in the decomposition estimated as the percentage of discharges concurrently identified within 0.5 ms tolerance by independent decompositions of two intramuscular signals (iEMG-iEMG) or one intramuscular and the surface EMG signals (iEMG-sEMG)

	Contraction level		
	5% MVC	7.5% MVC	10% MVC
iEMG–iEMG (%)	98.3 ± 1.1	97.4 ± 1.5	98.3 ± 0.4
iEMG–sEMG (%)	96.5 ± 4.2	92.4 ± 5.1	92.3 ± 6.0

Values are reported as means ± S.D. Results are shown for 60 s contractions at three force levels.

Figure 4*A* shows the discharge times of 10 motor units identified during a contraction at 5% MVC force. In this example, the first three motor units were identified from surface EMG decomposition and the other seven from the decomposition of the two intramuscular signals. Figure 4*B* shows the smoothed discharge rates for the 10 motor units, which presented common oscillations from visual inspection. The peak of the cross-correlation between motor unit pairs calculated using the classic measure of common drive (De Luca *et al.* 1982) was in this example (5 s duration) 66.0 ± 12.0% and corresponded to an averaged time lag of −9.4 ± 60.1 ms (Fig. 4*C*). Principal component analysis was applied to the same set of discharge rates to investigate the dimensionality of the control signal. Figure 4*D* shows four principal components extracted from the recording. In this example, the first component accounted for 70.4% of the total variance whereas the second component explained only ∼8% of the variance.

The group data analysis confirmed the observations made for the representative example of Figure 4. The relative power of the FCC signal (average over all forces, using time intervals of 5 s for comparison with the common drive measure, 64.3 ± 10.2%) was significantly greater than the common drive index over the same contraction intervals (58.7 ± 15.9%; averaged time lag 2.6 ± 16.8 ms, $P < 0.05$). The two measures of correlation among discharge rates showed positive correlation ($R^2 = 0.29$, $P < 0.001$), as expected from the theoretical analysis (eqns (2) and (3)). These results indicated that the FCC signal resembled the entire set of discharge rates by a greater degree than the average correlation between pairs of discharge rates. Neither the common drive between motor unit pairs ($R^2 = 0.007$, $P = 0.73$) nor the relative power of the FCC signal ($R^2 = 0.08$, $P = 0.27$) was correlated with the CIS index of synchronization (0.73 ± 0.24; Table 2), calculated for each contraction as an average over all pairs of identified motor units.

The results presented above refer to the computation of the common drive index and FCC as averages over all the time intervals of 5 s duration during the 60 s contractions. This analysis was performed for direct comparison of the results with the method suggested in previous work for estimating the strength of common drive (De Luca *et al.* 1982). The values for the common drive index and FCC signal reported in the following refer to the direct computation over the entire recording interval of 60 s. This further analysis was performed to investigate the association between the FCC signal and force over the full contraction interval.

From the group data calculated over the 60 s recording interval, the FCC signal explained a significantly greater amount of variability in the smoothed discharge rates (44.2 ± 7.5%) compared with the second principal

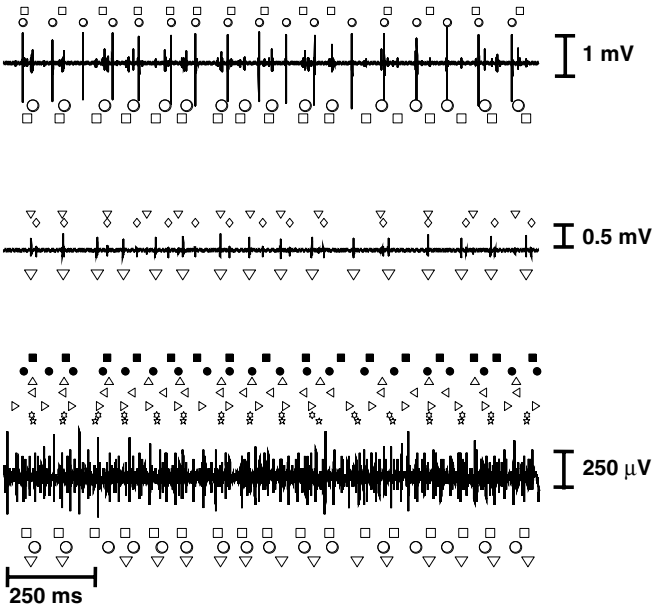

Figure 2. Comparison between intramuscular and surface EMG decomposition in the abductor digiti minimi muscle
For clarity, only one channel (6th row and 3rd column) from the surface EMG grid is depicted, and thus two intramuscular and one surface EMG signals are shown. Each symbol indicates a discharge of a motor unit as identified from each recording. Action potentials from the same motor units detected by at least two recording systems (three motor units in this case) are indicated with the same symbol (square, triangle and circle), reported below each signal trace. The contraction force was 5% MVC. iEMG: intramuscular EMG; sEMG: surface EMG.

Table 2. Motor unit characteristics for the three contraction force levels

	Contraction level		
	5% MVC	7.5% MVC	10% MVC
Mean discharge rate (pps)			
Beginning of the contraction (10 s)	11.4 ± 1.9	12.5 ± 2.3	14.3 ± 2.3
Mean discharge rate (pps)			
End of the contraction (10 s)	10.8 ± 2.3	11.6 ± 1.9	14.11 ± 2.2
Recruitment threshold (% MVC)	2.8 ± 1.7*	3.8 ± 2.8*	4.1 ± 3.3*
ΔFR (% MVC)	2.4 ± 1.6†	4.0 ± 2.3†	5.9 ± 3.3†
CoV for ISI (%)	16.6 ± 3.0+	20.4 ± 4.4	19.5 ± 4.7
Common drive index (%) (5 s)	61.5 ± 16.6	57.0 ± 13.7	57.7 ± 16.9
Strength first principal component (%) (5 s)	67.8 ± 12.9	63.9 ± 9.0	61.1 ± 8.8
Common drive index (%) (60 s)	37.5 ± 6.8	37.9 ± 10.1	36.9 ± 3.9
Strength first principal component (%) (60 s)	44.2 ± 6.7	45.7 ± 9.4	42.8 ± 7.8
Strength second principal component (%) (60 s)**	14.1 ± 3.4	12.0 ± 2.0	13.6 ± 5.0
Strength other components (%) (60 s)**	6.5 ± 1.6	6.9 ± 1.7	6.9 ± 2.3
Common input strength (CIS)	0.72 ± 0.22	0.78 ± 0.31	0.68 ± 0.15
Mean correlation (%)			
Correlation (*R*) between the first principal component and force ††	62.7 ± 10.9	62.9 ± 5.8	62.1 ± 15.0
Correlation (*R*) between motor unit discharge rates and force ††	41.3 ± 8.0	41.9 ± 8.6	40.8 ± 8.2

Values are group means ± S.D. *Significantly different among all contraction levels ($P < 0.001$). †Significantly different among all contraction levels ($P < 0.05$). +Significantly different between 7.5% MVC and 10% MVC ($P < 0.05$). ** Significantly different with respect to the first principal component ($P < 0.001$). †† Significantly different ($P < 0.001$). ΔFR: difference between the recruitment threshold and the target force in % of MVC; ISI: interspike interval; CoV: coefficient of variation.

component ($13.2 \pm 3.5\%$) ($P < 0.001$) and the other components ($6.8 \pm 1.8\%$) (Table 2). The strength of the FCC signal calculated over the entire recording interval was higher ($P < 0.001$) compared with the peak values of the cross-correlation functions for pairs of motor units computed over the same interval ($37.4 \pm 7.2\%$; Table 2).

Figure 5*A* shows a representative comparison between the FCC signal of the set of motor unit discharge rates and the force signal. From visual inspection, the two signals have similar low-frequency oscillations and in this example the peak value of their cross-correlation function was 61.5%. For comparison, Fig. 5*B* shows the force and the envelope of the surface EMG, which were correlated, in this example, by only 35.0%. From the group data, the peak of the cross-correlation between the FCC and the force signal ($62.7 \pm 10.1\%$; Table 2) was greater than the average peak value of the cross-correlation function between the smoothed discharge rates of individual motor units and force ($41.4 \pm 7.8\%$; Table 2) ($P < 0.001$). This indicated that the FCC signal of the population of discharge rates explained better the motor output compared to the motor unit discharge rates individually.

The correlation between FCC and force depended on the type of window used to smooth the discharge rates. For example, when using as a window the function proposed by Fuglevand *et al.* (1993) for describing the motor unit twitch force (with contraction time = 90 ms) instead of the Hann window, the association between the FCC and force signal increased to $71.8 \pm 13.1\%$ (average over all contraction forces). The strength of the association further increased by varying the contraction time in order to maximize the correlation for each subject (results not shown). Thus, the FCC signal extracted with optimal smoothing windows explained most of the force fluctuations.

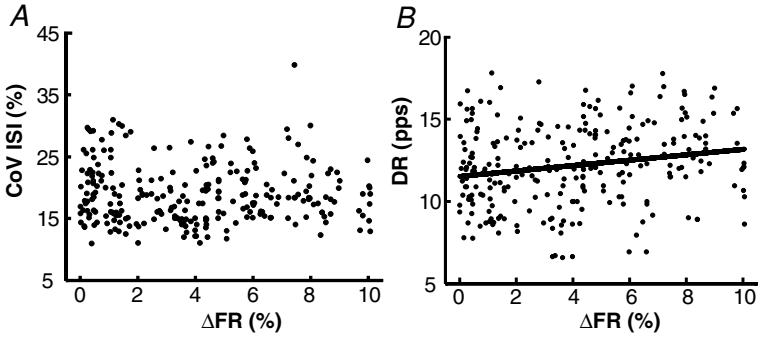

Figure 3. Association between ΔFR and discharge properties in the abductor digiti minimi muscle
A, scatter plot of the averaged coefficient of variation (CoV) for interspike interval (ISI) and ΔFR ($P > 0.05$). *B*, scatter plot of mean discharge rate (DR) and ΔFR ($R^2 = 0.04$, $P < 0.05$). Each circle denotes one motor unit and data are reported for all contraction levels and subjects.

Figure 6*A* shows a representative comparison between the FCC signal and the set of motor unit discharge rates used for the extraction of FCC (Fig. 6*A*). The value calculated using only one motor unit ($41.4 \pm 7.5\%$) was significantly lower than the values calculated using more than three motor units ($P < 0.001$) (Table 2 and Fig. 6*A*). On the contrary, when more principal components were added to the first, the correlation between the resultant signal and force decreased (Fig. 6*B*), being significantly lower when using six components or more with respect to one ($P < 0.001$). Moreover, the second component alone was weakly correlated with the force oscillations ($9.8 \pm 5.1\%$). Similar or lower correlation values were obtained for the other components. This indicated that only the first component (FCC) had an influence on the force fluctuations whereas the other principal components of the motor unit discharge rates did not influence the force produced.

The CoV for the FCC decreased with increasing the number of units, and values calculated using nine motor units ($8.7 \pm 2.8\%$) or more were statistically lower than those using one motor unit only ($6.5 \pm 3.5\%$; $P < 0.05$). Figure 7 reports the associations between the CoVs for the FCC, ISI, force signal and envelope of the surface EMG in one representative subject. In this example, there was a significant association between the CoV for force and the CoV for the FCC signal ($R^2 = 0.29$, $P < 0.001$) whereas the association was weaker between the CoVs for force and for the envelope of the surface EMG ($R^2 = 0.08$, $P = 0.08$). The results from the group data are reported in Table 3. The CoV for force was correlated to the CoV for the FCC in all subjects (R^2 range = 0.14–0.56; $P < 0.05$). Conversely, the CoV for FCC was correlated to the CoV for the surface EMG envelope in only four subjects (R^2 range = 0.02–0.47.; $P < 0.05$) and the CoV for the EMG envelope correlated to the CoV for force in only three subjects ($R^2 = 0.28.$; $P < 0.05$, $R^2 = 0.18.$; $P < 0.05$, $R^2 = 0.18.$; $P < 0.05$). Finally, the relation between the CoVs for ISI and force was the weakest and the result was significant in only one subject ($R^2 = 0.12$; $P < 0.05$).

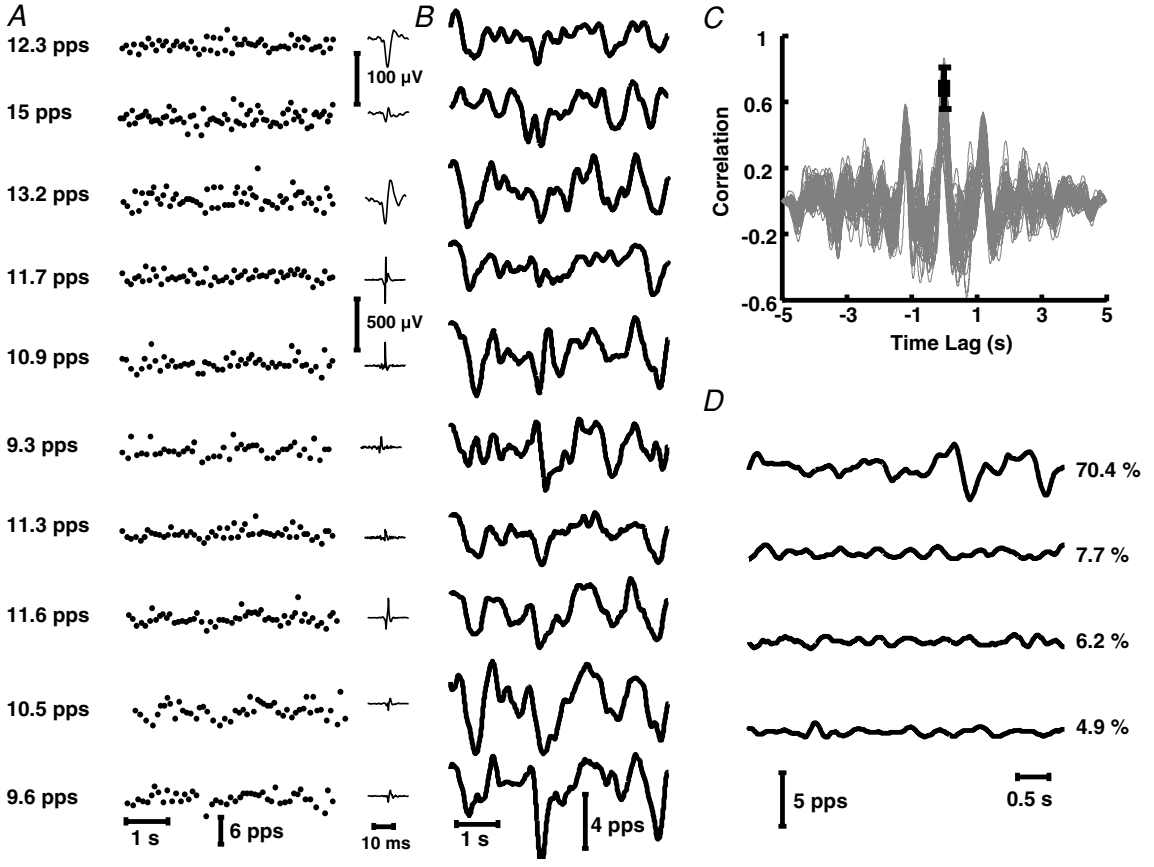

Figure 4. Extraction of principal components from motor unit discharge rates
A, instantaneous discharge rates for 10 motor units of the abductor digiti minimi muscle (the first 3 were identified from the surface EMG, the remaining 7 from the intramuscular recordings). The average discharge rates for the 10 motor units are reported on the left. *B*, smoothed discharge rates (Hann window of 400 ms duration). *C*, cross-correlation functions calculated for all pairs of the 10 motor units (average correlation: 0.66 ± 0.12; time lag: -9.4 ± 60.1 ms). *D*, first four principal components extracted from the set of detrended discharge rates shown in *B*.

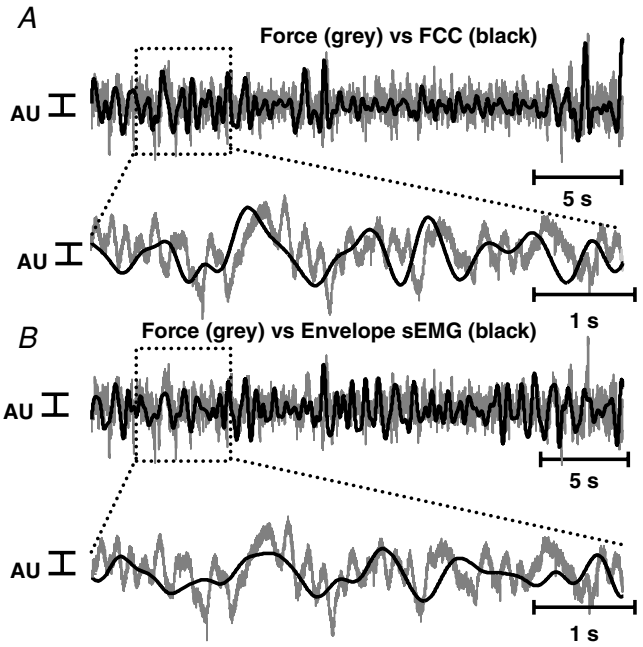

Figure 5. Representative comparison between the first common component of motor unit discharge rates and force
A, detrended force signal (grey) for a contraction at 7.5% MVC force of the abductor digiti minimi muscle and first common component (FCC) of the smoothed motor unit discharge rates (black). The peak of the cross-correlation between the two signals is in this example 61.5%. *B*, detrended force signal (grey) and envelope of the surface EMG (sEMG) signal (6th row and 3rd column of the grid) (black) for the same contraction as in *A*. The peak of cross-correlation between force and envelope of the surface EMG is 35.0%.

Figure 8*A* shows the coherence spectrum between the FCC and the force signal in one representative contraction at 7.5% MVC force. In this example, there was a strong linear relation between force and FCC for all frequency values in the range 0–4 Hz, which was the bandwidth for the FCC signal (−3 dB at 1.8 Hz). Figure 8*B* shows the coherence spectrum between force and envelope of the surface EMG for the same contraction. From the group data, the averaged maximal coherence value between FCC and force was significantly greater (0.70 ± 0.12) than the peak coherence value between the envelope of the surface EMG and force (0.44 ± 0.16) ($P < 0.05$).

To investigate the generalization of results to a larger muscle, measures were also performed on the tibialis anterior muscle. For this muscle, accurate spike trains could be identified for contractions up to 20% MVC; for this contraction level, the agreement between two intramuscular EMG decompositions was $97.2 \pm 2.1\%$ and between intramuscular and surface EMG decompositions was $93.4 \pm 6.1\%$. The results obtained by analysing the spike trains of 9 ± 1 motor units per contraction from the tibialis anterior were similar to those for the abductor digiti minimi muscle (Table 4). For example, the strength of the first principal component computed over one segment of 5 s duration and averaged over all subjects ($n = 8$) was $62.8 \pm 12.4\%$ at 10% MVC force and this component correlated with force by $58.1 \pm 13.9\%$ (Table 4). Similar results were obtained for higher contraction forces (15% and 20% MVC; Table 4). As for the abductor digiti minimi muscle, the strength of the correlation between FCC and force increased when using a window that resembled the

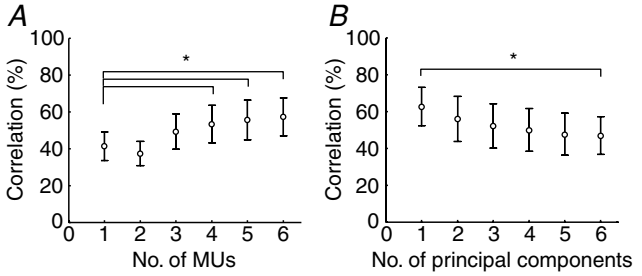

Figure 6. Association between the first common component and the force signal
A, mean (S.D.) correlation between the first common component (FCC) and the force (average over all contraction forces) in the abductor digiti minimi muscle, as a function of the number of motor units (MUs) used for the analysis. *Significantly different compared to the first value ($P < 0.001$). *B*, mean (S.D.) correlation between FCC and force in the abductor digiti minimi muscle, as a function of the number of components added together. *$P < 0.001$.

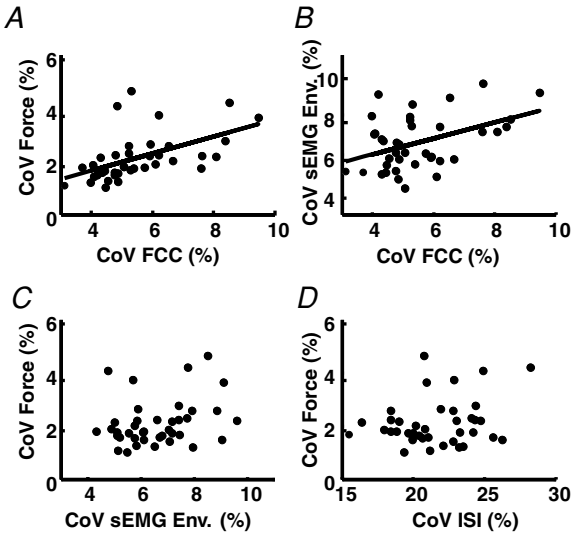

Figure 7. Relations between variability of force, the first common component, envelope of the surface EMG and interspike interval
Data are shown for the abductor digiti minimi muscle of one representative subject (all contractions are pooled). *A*, relation between CoV for force and for the first common component (FCC) signal ($R^2 = 0.29$, $P < 0.001$). *B*, relation between CoV for the FCC signal and envelope of the surface EMG ($R^2 = 0.18$, $P < 0.05$). *C*, relation between CoV for force and CoV for the envelope of the surface EMG ($R^2 = 0.08$, $P = 0.08$). *D*, relation between CoV for force signal and Cov for ISI ($R^2 = 0.06$, $P = 0.11$). Each circle corresponds to an interval of 4 s.

Table 3. R^2 and P values for the linear regression analyses between coefficient of variations (CoV) for force, first common component (FCC), envelope of the surface EMG and interspike interval (ISI)

Subject	CoV Force *vs.* FCC	CoV Envelope sEMG *vs.* FCC	CoV Envelope sEMG *vs.* Force	CoV Force *vs.* ISI
1	$R^2 = 0.29$, $P < 0.001$	$R^2 = 0.19$, $P = 0.05$	$R^2 = 0.09$, $P = 0.06$	$R^2 = 0.12$, $P < 0.05$
2	$R^2 = 0.53$, $P < 0.001$	$R^2 = 0.02$, $P = 0.45$	$R^2 = 0.002$, $P = 0.77$	$R^2 = 0.06$, $P = 0.15$
3	$R^2 = 0.29$, $P < 0.001$	$R^2 = 0.18$, $P < 0.05$	$R^2 = 0.08$, $P = 0.08$	$R^2 = 0.06$, $P = 0.11$
4	$R^2 = 0.56$, $P < 0.001$	$R^2 = 0.38$, $P < 0.001$	$R^2 = 0.28$, $P < 0.05$	$R^2 = 0.15$, $P = 0.05$
5	$R^2 = 0.14$, $P < 0.05$	$R^2 = 0.23$, $P < 0.05$	$R^2 = 0.05$, $P = 0.25$	$R^2 = 0.01$, $P = 0.56$
6	$R^2 = 0.50$, $P < 0.001$	$R^2 = 0.47$, $P < 0.001$	$R^2 = 0.18$, $P < 0.05$	$R^2 = 0.003$, $P = 0.70$
7	$R^2 = 0.54$, $P < 0.001$	$R^2 = 0.02$, $P = 0.48$	$R^2 = 0.18$, $P < 0.05$	$R^2 = 0.03$, $P = 0.7$
8	$R^2 = 0.41$, $P < 0.001$	$R^2 = 0.10$, $P = 0.29$	$R^2 = 0.06$, $P = 0.17$	$R^2 = 0.07$, $P = 0.11$

Values are reported for each subject pooling all contraction levels. CoV: coefficient of variation. FCC: first common component. sEMG: surface EMG. ISI: interspike interval.

twitch force instead of the Hann window (average of all contraction forces, 68.3 ± 15.7%).

Discussion

A signal has been extracted as a linear projection of the smoothed discharge rates of populations of motor neurons, identified by the decomposition of intramuscular and surface EMG recordings. This signal, which is the first principal component of the multivariate measure of discharge rates, explained a large portion of the total variance of the discharge rates and showed high correlation with the force output in two muscles. Adding other components to the first did not improve the correlation with force, and thus one component described the force fluctuations in the best way among the linear transformations of the ensembles of motor unit discharges.

For this study, it was necessary to estimate accurately the discharge trains of more motor units than is usually analysed in human studies. To overcome the limitation of a relatively small number of identified motor units of previous studies (De Luca *et al.* 1982; Stashuk, 2001), we have applied both intramuscular EMG and high-density surface EMG, which were decomposed with state-of-the-art and validated methods (Holobar & Zazula, 2004; McGill *et al.* 2005). The average number of motor units per contraction whose spike trains could be identified in the two muscles was ∼9, relatively high

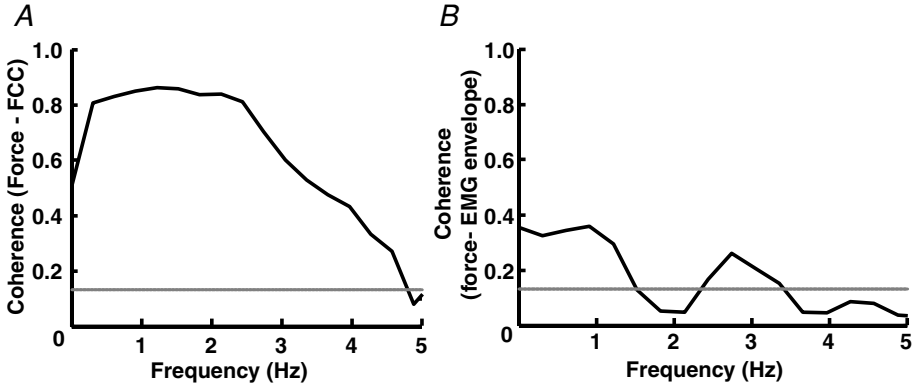

Figure 8. Representative coherence spectra
A, coherence spectrum between the force and the first common component in the abductor digiti minimi muscle of one representative subject. Values are above the confidence level (grey line) in the frequency interval 0–4 Hz. *B*, coherence spectrum between force and envelope of the surface EMG (one channel at the 6th row and 3rd column) for the same contraction. The contraction force was 7.5% MVC.

Table 4. Motor unit characteristics for the three contraction force levels in the tibialis anterior muscle

	Contraction level		
	10% MVC	15% MVC	20% MVC
Mean discharge rate (5 s) (pps)	11.9 ± 3.7	11.2 ± 1.6	13.8 ± 3.0
CoV for ISI (%)	15.4 ± 8.8+	23.2 ± 7.7	21.9 ± 6.1
CoV for FCC (%)	10.1 ± 9.0	12.4 ± 8.6	11.9 ± 4.7
CoV for Force (%)	1.8 ± 0.9	1.2 ± 0.5	1.8 ± 0.7
Common Drive Index (%) (5 s)	47.5 ± 14.3	41.8 ± 17.0	38.3 ± 7.4
Strength first principal component (%) (5 s)	62.8 ± 12.4	56.4 ± 13.1	59.7 ± 6.5
Strength second principal component (%) (5 s) **	19.6 ± 7.6	25.0 ± 10.4	24.7 ± 7.1
Strength other components (%) (5 s) **	8.6 ± 2.4	7.9 ± 3.1	7.8 ± 3.2
Mean correlation (%)			
Correlation (*R*) between the first principal component and force ††	58.1 ± 13.9	51.7 ± 12.6	52.4 ± 10.9
Correlation (*R*) between motor unit discharge rates and force ††	48.1 ± 8.5	45.5 ± 14.5	39.4 ± 11.3

Results are reported for 9 ± 1 motor units per contraction. Values are group means ± S.D., $n = 8$ subjects, for 10% MVC, 15% MVC and 20% MVC. Each value has been calculated over one epoch of 5 s for each contraction level averaged over all subjects. ISI: interspike interval; CoV: Coefficient of variation. +Significantly different between 10% MVC and 15% MVC and between 15% MVC and 20% MVC ($P < 0.05$); **Significantly different with respect to the first principal component ($P < 0.001$); ††Significantly different ($P < 0.05$).

compared to previous studies on common drive (De Luca *et al.* 1982, Adam *et al.* 1998, Erim *et al.* 1999). For these units, the decomposition accuracy was proven to be high (Table 1).

It was previously shown that the smoothed discharge rates of the active motor units show a degree of correlation during a contraction (De Luca *et al.* 1982). In this study, the first principal component of the entire set of motor unit discharge rates accounted for most of the variance (Tables 2 and 4). Moreover, the first component alone correlated to the force signal by a greater degree than when adding more components (Fig. 6). These results prove that the low-frequency oscillations of the discharges of motor neurons are well represented by a one-dimensional neural control signal. The strength of common oscillations in the motor neuron pool, expressed as the percentage of the variance described by the FCC signal, showed moderate to high correlation with a common drive index previously proposed (De Luca *et al.* 1982). This result was expected since both techniques describe the correlation between smoothed discharge rates. However, the relative power of the FCC signal represents the global association between motor unit discharges when considering all units together whereas the common drive index previously proposed analyses the units in pairs. Moreover, the method proposed in this study provides not only an indication of the strength of common activity among motor units (De Luca *et al.* 1982) but also a signal as a function of time that represents the overall common low-frequency oscillations in discharge of the identified motor units.

The signal extracted by principal component analysis from the detected motor unit discharges was compared with the force signal. The force output can be modelled as the convolution of the neural drive signal to the muscle and the average force twitch of the active motor units. The convolution by the average force twitch corresponds to a low-pass filtering of the neural drive signal, and thus it is expected that only the low-frequency components of the neural signal are effective in determining the characteristics of the generated force. Since the FCC was extracted from low-pass filtered discharge rates, it represented not only the common low-frequency oscillations of the population of motor units but also the force output. Accordingly, the FCC showed a correlation with force of ∼60% in both muscles, which is a greater value compared with the correlation values observed between individual motor units and force in this (Tables 2 and 4) and previous studies (De Luca *et al.* 1982). Moreover the other components alone showed negligible correlation with the force oscillations. When the discharge rates were smoothed with a window similar to the average twitch, the FCC resembled force with correlation of ∼70% in both muscles. The high correlation between FCC and force, especially when using a window that resembled the motor unit twitch force, indicates that the extracted signal explained most of the motor output, in agreement with the hypothesis that only the low-frequency components of the neural drive have an influence on the generated force and that one signal well represents the activity of the identified motor units.

Interestingly, the FCC signal resembled the force to a high correlation degree despite the fact that the actual sample of motor units, although being larger than in previous studies, was presumably small with respect to the number of active motor units. For example, the abductor digiti minimi muscle has ∼380 motor units (Santo Neto *et al.* 1985). According to the recruitment model proposed by Fuglevand *et al.* (1993), ∼150 of these motor units should be active in this muscle at 5% MVC. Similarly, in the tibialis anterior muscle there are ∼445 motor units

(Feinstein *et al.* 1955) and ∼240 of them should be active at 10% MVC, according to similar calculations (Fuglevand *et al.* 1993). Thus, the set of detected units in this study corresponded presumably to ∼5% of the number of active units. The observation that FCC computed from this relatively limited set of motor units, was correlated with the force for more than 70%, further supports the conclusion that the dimensionality of the control is very low, and thus a small number of spike trains is sufficient for extracting a neural component that well explains the motor output. The observation that the extracted FCC did not perfectly correlate with force ($R < 100\%$) was also expected because the transformation of each spike train in force occurs with a different twitch shape whereas the FCC is obtained by using the same window for all motor units.

In agreement with the high correlation with the force signal, the CoV for the FCC was strongly associated with the CoV for force for all contraction forces (these results were presented only for the abductor digiti minimi muscle). Conversely, the CoV for the ISI of the individual motor units was poorly correlated with the CoV for force. Simulation models have demonstrated that significant changes in the CoV for ISI may have a marked effect on the force steadiness (Enoka *et al.* 2003). However, the results from experimental studies are controversial and show only a weak association between force steadiness and CoV for ISI (Mottram *et al.* 2005). The results of this study further confirm that for the moderate force levels analysed, the CoV for ISI has a small influence on force fluctuations, especially when compared to the low-frequency oscillations in the motor unit discharge rates, as revealed by the FCC. This result is a consequence of the severe low-pass filtering of the neural signal for transduction into force. The CoV for ISI, which is due to the synaptic noise and its interaction with the time course of the post-spike afterhyperpolarization phase of the motor neuron (Matthews, 1996), constitutes a high-frequency component which is mostly filtered by the convolution of the discharge rates with the twitch forces and, when the number of active units is large, by summation of force contributions from different units.

In addition to the correlation between low-frequency components of the discharge rates, in the abductor digiti minimi muscle, we also analysed the degree of short-term synchronization among motor units (results not reported for the tibialis anterior). The CIS index of synchronization was relatively high for the hand muscle analysed, in agreement with previous studies (Semmler *et al.* 1997; Farina *et al.* 2008). However, CIS values were not correlated to the common drive index or to the strength of the FCC signal. This result is in agreement with a previous investigation on synchronization and common drive (Semmler *et al.* 1997) and confirms that the two types of correlation (synchronization among discharges and low-frequency common oscillations) have different origins.

The envelope of the surface EMG showed a weak correlation with both the FCC signal and force (Fig. 5*B*). Moreover the peak of the coherence spectrum between the envelope of the surface EMG and force was significantly lower than between FCC and force (Fig. 8). The surface EMG is generated from the neural drive signal by convolution of the spike trains with single motor unit action potentials. The model of generation is the same as for force but the filtering function is different. Bipolar motor unit action potentials have average value equal to zero and thus constitute the impulse response of high-pass filters, contrary to the twitch forces. This generates amplitude cancellation in the surface EMG (Farina *et al.* 2008) that hinders the association between neural drive to the muscle and amplitude of the surface EMG. These theoretical considerations were confirmed by the experimental results of this study (Figs 5, 7 and 8).

The main results of the study were similar in both muscles investigated. In both muscles, the multivariate smoothed discharge rates could be described by the FCC signal, whereas the other principal components had smaller influence; moreover, the extracted signal correlated with force to a similar degree for both muscles. This similarity was expected since the generated muscle force is the sum of the filtered spike trains (with twitch force as impulse response) and the proposed FCC signal is generated in a similar way. Variations in the degree of common drive among muscles (De Luca *et al.* 2009) would influence the strength of the first principal component, which is an index of common drive (eqns (2) and (3)), but to a lesser extent the association of the FCC signal with force.

In conclusion, this study shows that the ensemble of low-frequency oscillatory components of motor unit discharge rates can be represented by a one-dimensional signal, obtained by linear transformation of the smoothed discharge rates, which explains most of the force oscillations.

References

Adam A, De Luca CJ & Erim Z (1998). Hand dominance and motor unit firing behaviour. *J Neurophysiol* **80**, 1373–1382.

Davey NJ, Ellaway PH & Stein RB (1986). Statistical limits for detecting change in the cumulative sum derivative of the peristimulus time histogram. *J Neurosci Methods* **17**, 153–166.

De Luca CJ & Erim Z (2002). Common drive in motor units of a synergistic muscle pair. *J Neurophysiol* **87**, 2200–2204.

De Luca CJ, Gonzalez-Cueto JA, Bonato P & Adam A (2009). Motor unit recruitment and proprioceptive feedback decrease the common drive. *J Neurophysiol* **101**, 1620–1628.

De Luca CJ, LeFever RS, McCue MP & Xenakis AP (1982). Control scheme governing concurrently active human motor units during voluntary contractions. *J Physiol* **329**, 129–142.

Ellaway PH (1978). Cumulative sum technique and its application to the analysis of peristimulus time histograms. *Electroencephalogr Clin Neurophysiol* **45**, 302–304.

Enoka RM, Christou EA, Hunter SK, Kornatz KW, Semmler JG, Taylor AM, *et al*. (2003). Mechanisms that contribute to differences in motor performance between young and old adults. *J Electromyogr Kinesiol* **13**, 1–12.

Erim Z, Beg MF, Burke DT & de Luca CJ (1999). Effects of aging on motor-unit control properties. *J Neurophysiol* **82**, 2081–2091.

Farina D, Cescon C, Negro F & Enoka RM (2008). Amplitude cancellation of motor-unit action potentials in the surface electromyogram can be estimated with spike-triggered averaging. *J Neurophysiol* **100**, 431–440.

Farina D, Holobar A, Gazzoni M, Zazula D, Merletti R & Enoka RM (2009). Adjustments differ among low-threshold motor units during intermittent, isometric contractions. *J Neurophysiol* **101**, 350–359.

Feinstein B, Lindegard B, Nyman E & Wohlfart G (1955). Morphologic studies of motor units in normal human muscles. *Acta Anat (Basel)* **23**, 127–142.

Fuglevand AJ, Winter DA & Patla AE (1993). Models of recruitment and rate coding organization in motor-unit pools. *J Neurophysiol* **70**, 2470–2488.

Heckman CJ & Enoka RM (2004). Physiology of the motor neuron and the motor unit. In *Clinical Neurophysiology of Motor Neuron Diseases. Handbook of Clinical Neurophysiology*, ed. Elisen A, pp. 119–147. Elsevier.

Henneman E, Somjen G & Carpenter DO (1965). Excitability and inhibitability of motoneurons of different sizes. *J Neurophysiol* **28**, 599–620.

Holobar A, Farina D, Gazzoni M, Merletti R & Zazula D (2009*a*). Estimating motor unit discharge patterns from high-density surface electromyogram. *Clin Neurophysiol* **120**, 551–562.

Holobar A & Zazula D (2004). Correlation-based decomposition of surface electromyograms at low contraction forces. *Med Biol Eng Comput* **42**, 487–495.

Holobar A, Minetto MA, Botter A, Negro F & Farina D (2009*b*). Decoding the activity of populations of motor neurons from multichannel surface and intramuscular EMG. *International Workshop and Conference on Human Reflexes*, Izmir, Turkey, p. 63

Ishizuka N, Mannen H, Hongo T & Sasaki S (1979). Trajectory of group Ia afferent fibres stained with horseradish peroxidase in the lumbosacral spinal cord of the cat: Three dimensional reconstructions from serial sections. *J Comp Neurol* **186**, 189–211.

Joliffe IT & Morgan BJ (1992). Principal component analysis and exploratory factor analysis. *Stat Methods Med Res* **1**, 69–95.

Lawrence DG, Porter R & Redman SJ (1985). Corticomotoneuronal synapses in the monkey: Light microscopic localization upon motoneurons of intrinsic muscles of the hand. *J Comp Neurol* **232**, 499–510.

Lemon RN & Mantel GW (1989). The influence of changes in discharge frequency of corticospinal neurones on hand muscles in the monkey. *J Physiol* **413**, 351–378.

Mambrito B & De Luca CJ (1984). A technique for the detection, decomposition and analysis of the EMG signal. *Electroencephalogr Clin Neurophysiol* **58**, 175–188.

Mannard A & Stein RB (1973). Determination of the frequency response of isometric soleus muscle in the cat using random nerve stimulation. *J Physiol* **229**, 275–296.

Matthews PB (1996). Relationship of firing intervals of human motor units to the trajectory of post-spike after-hyperpolarization and synaptic noise. *J Physiol* **492**, 597–628.

McGill KC, Lateva ZC & Marateb HR (2005). EMGLAB: An interactive EMG decomposition program. *J Neurosci Methods* **149**, 121–133.

Milner-Brown HS, Stein RB & Yemm R (1973). Changes in firing rate of human motor units during linearly changing voluntary contractions. *J Physiol* **230**, 371–390.

Mottram CJ, Christou EA, Meyer FG & Enoka RM (2005). Frequency modulation of motor unit discharge has task-dependent effects on fluctuations in motor output. *J Neurophysiol* **94**, 2878–2887.

Negro F & Farina D (2008). Common components in the discharge rates of populations of motor units in the abductor digiti minimi muscle. *2008 Abstract Viewer/Itinerary Planner*, Program No. 859.17/II17. Society for Neuroscience, Washington, DC.

Nordstrom MA, Fuglevand AJ & Enoka RM (1992). Estimating the strength of common input to human motoneurons from the cross-correlogram. *J Physiol* **453**, 547–574.

Person RS & Kudina LP (1972). Discharge frequency and discharge pattern of human motor units during voluntary contraction of muscle. *Electroencephalogr Clin Neurophysiol* **32**, 471–483.

Ralston HJ 3rd, Light AR, Ralston DD & Perl ER (1984). Morphology and synaptic relationships of physiologically identified low-threshold dorsal root axons stained with intra-axonal horseradish peroxidase in the cat and monkey. *J Neurophysiol* **51**, 777–792.

Santo Neto H, de Carvalho VC & Penteado CV (1985). Motor units of the human abductor digiti minimi. *Arch Ital Anat Embriol* **90**, 47–51.

Semmler JG, Nordstrom MA & Wallace CJ (1997). Relationship between motor unit short-term synchronization and common drive in human first dorsal interosseous muscle. *Brain Res* **767**, 314–320.

Semmler JG & Nordstrom MA (1999). A comparison of cross-correlation and surface EMG techniques used to quantify motor unit synchronization in humans. *J Neurosci Methods* **90**, 47–55.

Stashuk D (2001). EMG signal decomposition: How can it be accomplished and used? *J Electromyogr Kinesiol* **11**, 151–173.

Walker SG & Van Mieghem P (2008). On lower bounds for the largest eigenvalue of a symmetric matrix. *Linear Algebra and its Applications* **429**, 519–526.

Author contributions

The study was conducted at the "Center for Sensory-Motor Interaction" of Aalborg University, Aalborg, Denmark. F.N. and D.F. designed the study and collected the data. F.N. and A.H. analyzed the data. All authors interpreted the results and contributed to the drafting and revisioning of the manuscript. D.F. and A.H. raised the fundings for the study.

Acknowledgements

The authors are grateful to Klaus Mayntzhusen, Martin Nøhr Nielsen and Jacob Koch Pedersen (Aalborg University, Denmark) for performing preliminary data analyses. This study was supported by the European Project TREMOR (Contract no. 224051) (D.F.) and by the Marie Curie reintegration grant within the 7th European Community Framework Programme (iMOVE, Contract No. 239216) (A.H.).